Surface Electromyographic Signals as a Tool for Biomechanics and Muscle Coordination Analysis

Franck Quaine, Anton Dogadov, Christine Serviere, Natalia Lopez

Surface Electromyographic Signals as a Tool for Biomechanics and Muscle Coordination Analysis.

Introduction

The surface electromyographic signal (EMG[1]) is a recorded variation of electrical potential in a given point of the skin, created due to electrical activity of the muscle of interest. The electrical activity always accompanies muscle mechanical activity and may be used to analyze the latter. EMG is used in medicine, biomechanical studies, analysis of motor control strategies and rehabilitation. The purpose of this chapter is to present the bases of EMG signal generation physiology, EMG acquisition techniques and their limitations, as well as the possible applications of EMG signal in biomechanics and muscle coordination analysis. A reader, interested in learning more about electromyography can find a detailed and complete presentation of EMG in textbooks [1–4] and in survey article [5]. The detailed recommendations about the EMG acquisition procedure may be found in European project SENIAM recommendations [6] or more recent CEDE project [7].

Physiological bases of the surface electromyographic signal generation

The activity of the muscle as a whole is determined by activity of the motor units (MU) of the muscle, which are the smallest functional units of the motor system. Each MU consists of a set of extrafusal (standard) muscle fibers and an α-motor neuron, innervating these fibers. The number of fibers, innervated by the same motor neuron is known as an innervation number. Below we will show how the EMG signal is created, starting from the muscle fiber and finishing by a whole muscle.

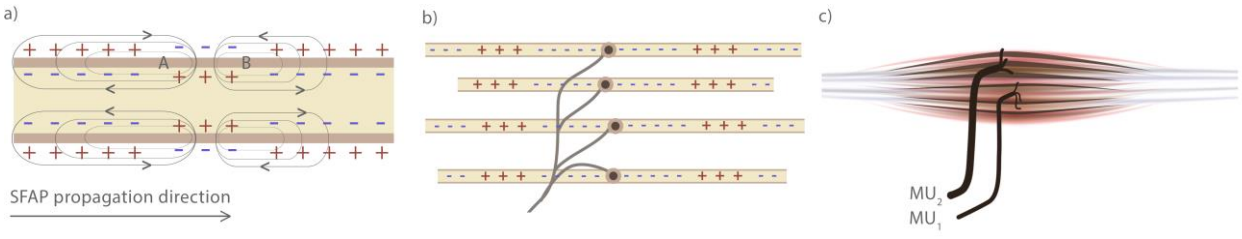

Figure 1. EMG generation. (a) A single fiber action potential (SFAP) generation. A depolarized zone in a muscle fiber, located between the letters A and B, propagates rightwards. The circular lines show the current flow around the depolarized zone, which consist in ionic and capacitive current. (b) A motor unit action potential (MUAP) generation. An activation from α-motor neuron propagates to underlying muscle fibers and creates action potentials, propagating in both sides from the innervation zone. A jitter between action potentials in different fibers is shown. (c) An EMG signal generation. Different MUs are recruited according to size principle, from smallest (MU_1) to largest (MU_2).

[1] The surface electromyographic signal may be denoted as sEMG, when one wants emphasize that the signal is recorded with surface electrodes, contrary to intramuscular recordings. In this chapter only the surface EMG will be discussed, therefore we will use an acronym EMG to denote the surface electromyographic signal.

The action potential of single fiber

The action potential arrives from motor neuron to a motor end plate (neuromuscular junction) of a muscle fiber, which is usually located in the middle of a fiber. It results in a local depolarization of the muscle-fiber membrane (the sarcolemma), creating a single fiber action potential (SFAP, Figure 1a). Next, two depolarized zones start to propagate along the muscle fiber from the neuromuscular junction towards both fiber endings. One depolarized zone has a length of few millimeters. In Figure 1a, one depolarized zone is shown between the letters AB. The velocity with which the action potential propagates depends principally on fiber type and diameter, and is called a conduction velocity (CV). The typical CV values are 3-5 m/s. When the single fiber action potential vanishes at the tendon junction, it generates a non-propagating burst. This phenomenon is known as *end-of-fiber* effect.

The depolarization zone is surrounded by electric current flow, which consists in ionic and conductive current (Noble, 1966). This electric current flow passes through by biological tissues, which act as volume conductor, and creates a SFAP "image", observed at the skin, which may be measured by surface electrodes [9].

The activation, arriving from a motor neuron, activates all muscle fibers, composing the same motor unit, which results in motor unit action potential generation.

The action potential of individual motor unit

The action potential arriving from a motor neuron separates to different branches (telodendria) and consequently activates all underlying muscle fibers. The activity of all muscle fibers of a MU forms motor unit action potential (MUAP). The activation arrives to all muscle fiber end plates almost simultaneously; however, the conduction time for different SFAPs may be different because of the differences in end-plate locations and SFAP propagation velocities. The latter are results of the variability of fiber diameters and lengths. Hence, the constituent SFAPs, generated by different fibers of the MU, are not perfectly synchronous. Consequently, the difference between from single fiber to MUAP is not simply the amplification of SFAP amplitude and the waveform of a MUAP is more complicated than a waveform of composing SFAPs. The muscle consists of different numbers of MUs, which may be of different type and size.

The resulting interferential pattern of a muscle

All active MUs in the muscle contribute in creating an interferential pattern, which is a distribution of the potential on the skin. This spatial and temporal interference pattern is the result of many physiological and anatomical factors, among them the firing behavior of MUs and

fiber type composition of the muscle [5]. When these potentials are recorded from the skin, the obtained signal is called a surface electromyographic signal. The EMG is a sum of MUAP train from different MUs of the muscle, recruited according to the size principle from smallest to largest. The surface EMG signal from the muscle is acquired by means of surface electrodes, according to a procedure, presented in the next section.

EMG signal acquisition methods

Below we briefly introduce the basis of surface EMG acquisition. The surface EMG signal is recorded by surface electrodes placed at the skin over the muscle of interest, therefore the surface electrodes are easier in use than intramuscular electrodes and their application is painless. According to use of conductive gel, the electrodes may be wet or dry. Wet electrodes contain a contact area, which is either already covered by a conductive gel (pre-gelled electrode) or must be covered with a gel by a user before application. Dry electrodes usually represent a metallic contact area, which is applied directly to the skin. Wet electrodes allow lower electrode-skin contact impedance; dry electrodes has a higher impedance and may be applied when the use of wet electrodes is not possible (e.g., prosthesis control).

The physics of surface electrode recordings

An electrode, either dry or wet, contains a conductive element, which is put in contact with an electrolyte. In case of wet electrodes, the electrolyte is a conductive gel, covering the electrode, which is, in turn, in contact with the electrolyte of the skin (e.g. a sweat, extracellular and intracellular fluid). In case of dry electrodes, the electrolyte is a physiological electrolyte of the skin. An electrode with electrolyte forms an electrochemical half-cell (Figure 2). The carries of charge are electrons in electrode and ions in electrolyte. The interface between the electrode and electrolyte forms an electrical double layer. The electrode side of the double layer is formed by the excess (or deficiency) of the electrons. The electrolyte side of double layer is formed by ions, cations (or anions). There is a distance between the two layers, because each ion as well as the electrode surface is covered by a shell of solvent molecules. Therefore, the double layer acts like a capacitor. In Figure 2 this capacitor is represented by C_{eg}. Besides the capacitive effects, redox reactions may be possible at the electrode surface, allowing the direct transfer of charge from the electrode to electrolyte and vice-versa. In Figure 2 this effect is represented by the resistance R_{eg}. The electrode for which only the capacitive effect occurs is called an ideal polarizable (polarized) electrode. The electrode, for which current passes freely through the electrode-electrolyte interface (only resistive effect occurs), is called an ideal non-polarizable electrode. Ideal polarizable and non-polarizable electrodes do not really exists, however, the electrodes, fabricated from the noble metals act close to ideal polarizable electrodes, and the

silver/silver chloride (Ag/AgCl) electrodes act close to ideal non-polarizable electrode. Finally, the half-cell potential occurs at the electrode-electrolyte interface. In Figure 2 this effect is represented by a DC-battery $E_{eg.}$

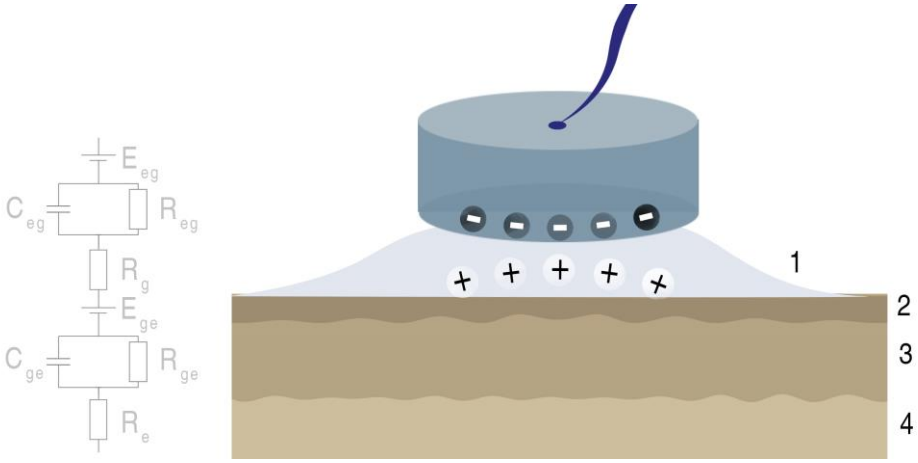

Figure 2. Wet surface electrode schematic view. 1 – gel, 2 – epidermis, 3 – derma, 4 – subcutaneous layer. The equivalent electric circuit is shown in the left. Electrode-gel interface: E_{eg} – the half cell potential, C_{eg}, R_{eg} – capacity and resistance of electrode-gel interface, R_g – resistance of gel. Gel-body electrolyte interface: E_{ge} – gel-body electrolyte potential, C_{ge}, R_{ge} – capacity and resistance of gel-body-electrolyte interface, R_e – resistance of dermis.

It should be noticed that there is a concentration difference between the ions in gel and body electrolyte in case of wet electrode use, which creates the gel-body electrolyte potential (E_{ge} in Figure 2) and also has an impedance (C_{ge}, R_{ge} and R_s in Figure 2).

The commonly used EMG recording consists in using one EMG channel by muscle. Below we describe the principle techniques for single-channel potential recording.

Single channel EMG recording.

An electrical potential in a given point of skin may be measured only relatively to another point on skin, therefore measuring EMG requires at least two electrodes, one placed over the muscle of interest and a second one, placed in the area with no muscle activity. However, EMG signal recording is usually performed inside a clinical or research environment, containing electric power cables (220 V/110 V of voltage alternating at 50 Hz/60 Hz according to a country).

These cables (phase and ground) create an additional potential on the body by means of electrical capacity of surrounding medium, e.g. the air and footwear. This potential, introduced by power cables, is considered the same in all points of the body (common mode). However, this potential may influence the EMG recording. To reduce this common mode signal the differential amplifiers are usually used, which requires three inputs: two differential inputs and a ground input. From the circuit design point of view, a differential amplifier is usually represented by an instrumentation amplifier. Therefore, recording a single channel EMG signal from one muscle

usually requires at least three electrodes. The differential amplifier intensifies the difference between two inputs, measured with reference to a ground electrode. These electrodes may be placed over the skin in different configurations, which are presented below.

Bipolar configuration

The most commonly used electrode configuration is a single differential (bipolar) electrode configuration. Bipolar configuration consists in two signal electrodes (Sig^a and Sig^b), placed along the muscle fiber direction. Both signals electrodes must be located between the innervation zone and muscle-tendon junction. A third, ground electrode is usually placed in the area with no EMG activity (e.g. a wrist). The EMG signal, measured in differential mode, represents a signal in the first electrode minus signal in a second electrode. Both signals are recorded with reference to a ground electrode. As the signal propagates from the innervation zone to muscle-tendon junction, passing through both electrodes, the electrode Sig^b receives a similar signal that the electrode Sig^a, but delayed in time. Making the difference between the signals on these electrodes results in subtracting the delayed version of the signal from the same signal. This subtraction, firstly, eliminates the common mode from power line, and, secondly, reduces no-propagating components of the signal which are similar at both electrodes (principally, the activity from distant muscles).

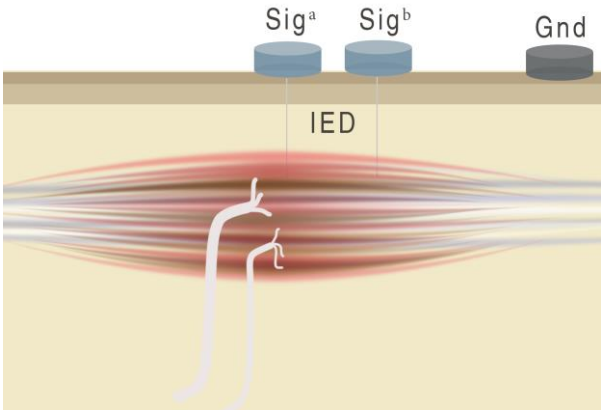

Figure 3. The schematic representation of a bipolar electrode placement. Two electrodes, Sig_a and Sig_b are located over the muscle of interest. IED is the interelectrode distance.

When choosing the size of electrode it should be noticed that increase of the electrode size reduces the impedance, but also reduces the electrode's selectivity. Indeed, the potential recorded by an electrode is an average of the potential over the electrode area. Hence, bigger the electrode is, larger is the averaging area and less is the electrode's selectivity. SENIAM suggest to use the surface electrodes with the maximal size of 10 mm in the direction of muscle fibers [6]. If one aims in recording the activity of individual motor units, the electrodes generally must be smaller.

The interelectrode distance (IED) is defined as the distance between the centers of the signal electrodes. SENIAM reports that the optimal IED is 20 mm, but it must be less than 1/4 of the muscle fiber length.

We recall that the electrode-electrolyte interface is characterized by a half-cell and gel-electrolyte potential, as well as the impedance of the electrode-gel and gel-electrolyte interfaces. The DC voltage created by a half-cell and gel-electrolyte potential may be compensate if both signal electrodes Sig^a and Sig^b are the same, therefore it is important to use both signal electrodes of the same material and form, and to treat the skin under both electrodes at the same manner. Moreover, if the impedance of two electrodes differs, the common-mode signal rejection quality will decrease. At the same time, these impedances must be kept as small as possible, which may be achieved by skin pretreatment. Thus, the skin must be pretreated before the electrode application to minimize the impedances of both electrode-electrolyte interfaces and to equalize them. The standard skin treatment consists in washing the skin with soap, razing the hair and rubbing the skin with medical abrasive paste.

Finally, the displacement of the electrode causes the modification of the electrical double layer, which results in movement artefacts in the signal. To avoid them, the electrode cables must be fixed on the skin with the double sided tape or elastic band.

We presented the principles of EMG signal acquisition in a bipolar configuration. However, the other configuration may be also used to record an EMG signal. Below we present them briefly.

Monopolar configuration

In a monopolar configuration, only one electrode is placed over the muscle (Figure 5a, left panel). This configuration usually requires two additional electrodes, reference and ground. The reference and the ground electrodes are usually placed in the area with no EMG activity. The signal, recorded by EMG channel in such configuration represents muscle activity recorded by a signal electrode minus the signal in reference electrode. All signals are recorded with reference to a ground electrode. In this case, subtracting a signal from the reference electrode results only in reducing the common mode, introduced by power line. The monopolar configuration may be useful if one is interested in a MUAP form analysis, because this configuration does not change the signal form, as bipolar configuration.

Double differential and Laplacian configurations

Moreover, more sophisticated electrode system configuration may be proposed, for example, a double differential (Figure 5c, left panel). and Laplacian configuration. Their principle is similar with differential configuration. In case of double differential configuration, three signal electrodes are used (Sig^a. Sig^b and Sig^c in Figure 5c). The output signal is

represented as a sum of signal from lateral electrodes, Sig^a and Sig^c, minus double signal in a central electrode Sig^b. All the signals are recorded with reference to a ground electrode. In case of Laplacian configuration, five signal electrodes are used (located as a cross around the central electrode), and the output signal is represented as a sum of signal from lateral electrodes minus a signal in a central electrode, multiplied by four. All signals are recorded with reference to a ground electrode. The advantage of these techniques is the higher reduction of interfering signals from distant sources.

We presented the methods of single-channel acquisition, which may be used to obtain one signal from the muscle. When several electrodes are used to record the signals from several zones they usually have the same ground electrode (or ground and reference electrode in case of monopolar recordings). More advanced techniques consist in using a high number of electrodes, placed over the area of interest as a column or a matrix (high density surface EMG, HD-EMG). These electrodes provide a multichannel signal from the area of interest.

HD-EMG recording.

The matrix of monopolar electrodes (Figure 4) can represent an activity of the muscle as a whole, providing information about the potential in high number of individual locations over the skin. The size of electrodes in the matrix may be sufficiently small to distinguish the activity of individual motor units.

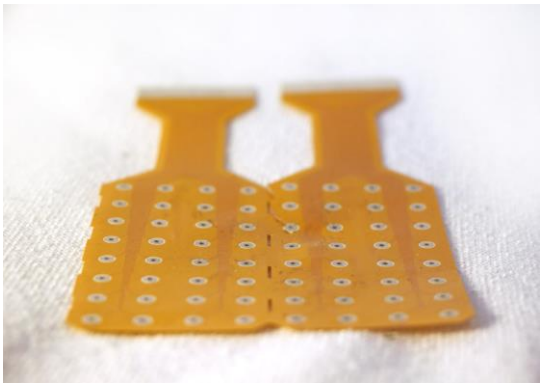

Figure 4. The 8-by-8 HD-EMG matrix with 10 mm interelectrode distance, developed in LISiN (courtesy of LISiN laboratory, Politecnico di Torino).

The signal from electrode matrix provides information about the change of the potential in both time and in space. Furthermore, we will call “a map” the recorded distribution of the potential over the space, either instantaneous or averaged during a certain time window. Hence, the Nyquist criterion must be satisfied in both frequency domain (by choosing appropriate sampling frequency) and spatial frequency domain (by choosing appropriate interelectrode distance). Moreover, the electrodes act like filters in spatial domain. Hence, the form of electrode

changes the transfer function of the filter and has an important influence on recorded potential map [10].

An HD-EMG matrix usually represents an array of electrodes in monopolar configuration, therefore it requires a reference and a ground electrode. An array of monopolar signal, recorded with an HD-EMG matrix may be numerically transformed into an array of bipolar, double differential or Laplacian signals by summation of the weighed signals from the monopolar array.

EMG signal preprocessing

The EMG signal is converted to digital form by analog-to digital converter with a sampling frequency which is usually fixed at 1000 Hz for general purpose application. If one is interested in MUAP waveform analysis, the sampling frequency must be up to 10 000 Hz. The digital signal may be filtered with a digital low pass filter with a cut-of frequency 10-20 Hz to remove the baseline drift and reduce the movement artefacts. As it was mentioned above, the difference between electrode-electrolyte interface impedance among the electrode results in decrease of common-mode reduction performance. Thus, to reduce the remaining 50 Hz (60 Hz) and its harmonics from the signal several techniques may be used. One possibility is to use a notch filter. However, if the reader is interested in analyzing the propagation of individual MUAPs it is recommended to use instead an adaptive filter or spectral interpolation, which does not modify the phase spectrum of the signal.

Crosstalk reduction methods

Several approaches may be used to reduce the crosstalk from different muscles. Among them, there are instrumental methods, such as using differential and double differential electrode systems, which reduce the amount of signals captured from distant muscles. Moreover, a special attention must be payed to proper electrode placement. From the other hand, there are computational methods, such as blind source separation methods (BSS). These methods may perform additional crosstalk reduction once the instrumental methods were applied.

Instrumental methods

Differential and double differential electrodes reduce crosstalk introduced by deeper muscles with reference to monopolar recordings. These methods reduce the signal from distant sources.

To illustrate how the acquisition mode influences the signal-to-crosstalk ratio, we simulated two overlapping muscles, using the simulator developed by Farina and Merletti (2001). Each muscle was represented by a set of 30 MU with parallel fibers. One muscle was deeper then another; the muscle centers were located at 4 mm and 9 mm depth. The fiber

direction was -10° for the first muscle and 10° for the second one. We simulated EMG signals in monopolar, bipolar and double differential configuration from these muscles. Two muscles were simulated to be active alternately during the same time.

We considered that the superficial muscle was a muscle of interest and the deep muscle was an interfering muscle. Thus, we calculated the signal-to-crosstalk ratio as the ratio of the superficial muscle signal power to the deeper muscle signal power:

$$SCR = 10\lg \frac{\sum_{k=N+1}^{2N} \left(x_k\right)^2}{\sum_{k=1}^{N} \left(x_k\right)^2}, \quad (1)$$

Where x_i is the k-th sample of the signal x, which may be a monopolar, bipolar and double differential signal. The deeper muscle was active for the values of i from 1 to N, and the superficial muscle was active for i values from N+1 to 2N.

We also calculated a gain of each acquisition mode with reference to a monopolar one, which was calculated as a gain difference in current mode and monopolar mode. Figure 5 illustrates the signal in monopolar (a), bipolar (b) and double differential (c) configurations. Solid line shows the envelope of the rectified EMG signal (in gray).

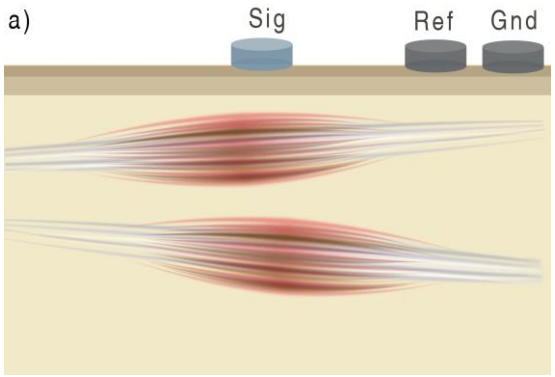

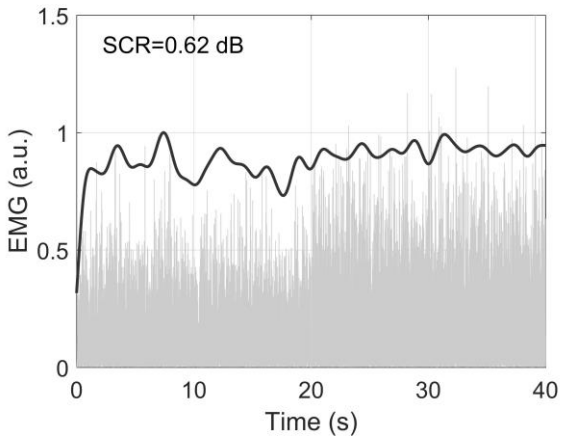

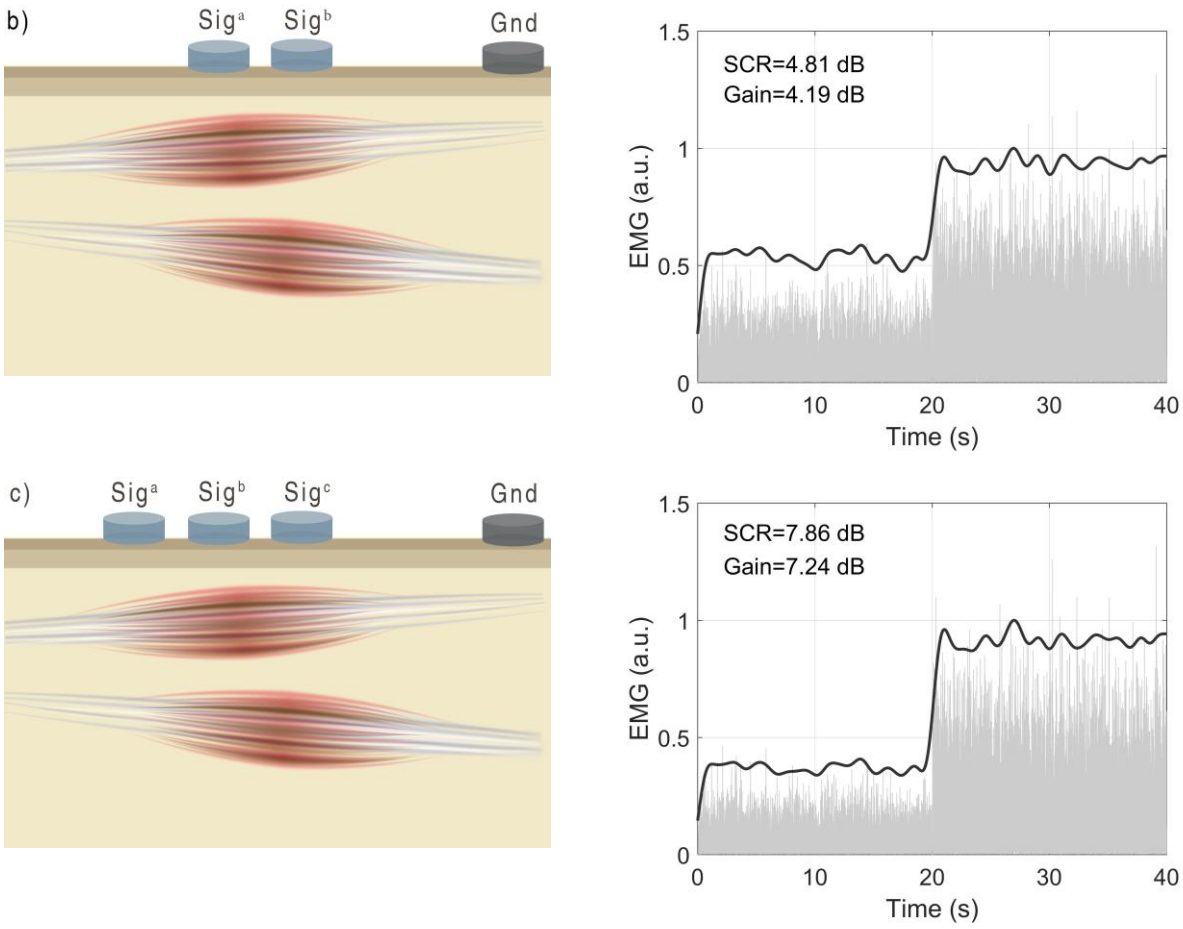

Figure 5. The signal from two overlapping muscles in monopolar (a), bipolar (b) and double differential (c) configuration. It may be seen how the signal from the deeper muscle is attenuated in bipolar and double differential configuration with reference to monopolar configuration.

It can be seen from the figure that the bipolar and double-differential configuration provides higher attenuation of the signal from deep muscle than the monopolar configuration (SCR 4.61 dB and 7.86 dB vs 0.62 dB).

Designed filters may also be effective to reduce crosstalk on sampled signals. Differential and double differential methods as well as Laplacian filters can be used as selective filters with a small detection volume on the muscle of interest. However, in this way, to remove the potential coming from the nearby muscles, also most of the EMG produced by the muscle under investigation may be discarded. Above classical spatial filters, Mesin [12] proposed an optimal spatio-temporal filter (OSTF). Its coefficients are computed on a training set to optimize the signal to crosstalk ratio on the set.

Blind source separation

Blind source separation (BSS) aims at recovering source signals s from several mixtures when no a priori information is available on source properties (source spatial position etc.). To reduce the crosstalk from neighbor muscles, BSS is applied to recorded signals x that are

supposed to be transformed vectors of source signals s and each muscle is thought to be a source. Most of mixing transformations are supposed to be linear instantaneous or linear convolutive.

A linear instantaneous model can be used in the case of small muscles located close to each other [13]. However, validity of the instantaneity hypothesis is very sensitive to electrode location [14]. Merletti [15] explained the limitations of the instantaneous model by a convolutive effect of a volume conductor and by action potential propagation.

To estimate the source signals independent component analysis (ICA) is usually used [16]. ICA was first used to the decomposition of the signal of a single muscle into a number of motor unit action potentials MUAP before to be used to the crosstalk problem (several muscles mixed in the observations) [17]. ICA is a group of methods that lead to the transformation of a set of recordings into a set of independent source signals. ICA could be performed in time-domain if instantaneous model is chosen, or in time frequency domain in the case of convolutive model.

In both cases, the time or frequency observations vectors x are modeled as:

$$\mathbf{x} = \mathbf{A}\mathbf{s} + \mathbf{N}, \quad (2)$$

where N represents an additive white noise vector and A is an unknown real or complex mixing matrix.

Principal Component Analysis (PCA) is usually used as a first step to reduce the data space by projection in the source subspace by spatial whitening [18–20]. The whitening matrix W is estimated from data and the whiten observations z are therefore linked to the sources by a remaining unknown unitary matrix $\mathbf{\Pi}$:

$$\mathbf{z} = \mathbf{W}\mathbf{x} = \mathbf{\Pi}\mathbf{s}, \quad (3)$$

ICA looks for a demixing matrix $\mathbf{\Pi}^{-1}$ such that the estimated sources $\mathbf{\Pi}^{-1}\mathbf{z}$ are not only uncorrelated but also independent. Different types of diversity can be used to perform the estimation of the unitary matrix $\mathbf{\Pi}^{-1}$ and test independence: non-gaussianity (Infomax [21], FastICA [22], EFFICA, JADE [23], EBM, RADICAL), sample dependence (AMUSE, SOBI [18], WASOBI) or nonstationarity [24,13]. Many studies use the first type of diversity to perform BSS on EMG signals. Naik [25] performed a comparison of JADE, FastICA and Infomax ICA methods. They applied ICA on EMG signals, preliminary decomposed into intrinsic mode functions by the ensemble mode decomposition algorithm. The separated sources were used to classify each EMG recording as normal or pathological one. The classification performance was significantly higher when FastICA method was used.

The methods, using the second type of diversity were first developed by Belouchrani (SOBI) [18] and look for uncorrelated sources at different time delays. The BSS technique based

on second-order moments SOBI assumes instantaneous mixtures. Jiang and Farina [26] proposed an extension of SOBI for the case of sources being delayed in the mixtures and used it to separate the EMGs. The proposed method was based on the transformation of the delayed mixtures to the mixtures of original sources and their first derivatives by the first-order Taylor approximation. The method is applicable only to mixtures with small delays.

BSS using nonstationarity diversity was first developed by Pham and Cardoso [24]. Non stationarity is taken into account by joint diagonalization of correlation matrices [24] or spectral matrices [27]. It is very popular in audio separation and Farina *et al* [13]. applied the concept to EMGs. They investigated linear instantaneous mixtures of EMG signals using joint diagonalization of Spatial Time-Frequency Distributions.

However, blind source separation methods rely on assumptions that may not be totally valid for some EMG recordings. A necessary hypothesis concerns the spatial diversity which roughly means that the mixing process is invertible, whatever it is matrix or filters matrix. This means that when using a BSS method, both estimated sources and demixing matrices must be checked to validate the results.

In second-order methods using joint diagonalization of correlation matrices, spectral matrices or other, a relying assumption is that correlation functions or spectra of sources are different enough to bring additive information in the joint diagonalization. If not, it leads to error in the estimation of the unitary matrix $\mathbf{\Pi}$. The waveforms issued from two distinct muscles may be very close as the physiological process is the same. However, some differences may appear if the muscle widths and so the fibers number or forces are different enough.

Methods based on source independence [14] may also fail in separation of the signals from individual muscles because each muscle consists of motor units, which also may be considered as individual sources by a source separation algorithm. Hence, there is no evidence if the separated sources are the signals produced by different muscles or from different motor units (MU) of the same muscles.

Moreover, the question if the EMG signals produced by different muscles are always statistically independent remains open. They may be temporally overlapped that could make the sources no more independent, because the MUAPs' waveforms are similar. This can happen in case of high force levels when the MU number increases.

Below we show the results of convolutive JADE (performed in frequency domain) applied on simulated signals. The convolutive JADE was applied on two simulated signals, x_1 and x_2, from two monopolar electrodes, Sig 1 and Sig 2, located in direction, perpendicular to muscle fibers (Figure 6). Two sources, s_1 and s_2, were estimated as which may be related with activities of two muscles. For two sources, the signal to crosstalk ratios were calculated:

$$SCR_1 = 10\lg\frac{\sum_{k=N+1}^{2N}\left(s_{1k}\right)^2}{\sum_{k=1}^{N}\left(s_{1k}\right)^2}, \quad (4)$$

$$SCR_2 = 10\lg\frac{\sum_{k=1}^{N}\left(s_{2k}\right)^2}{\sum_{k=N+1}^{2N}\left(s_{2k}\right)^2}.$$

SCR_1 is the SCR of the first source, related to the superficial muscle, which is calculated as the ratio of the power of the superficial muscle contribution to this source to the power of the deep muscle contribution to this source. SCR_2 is the SCR of the second source, related to the deep muscle, which is calculated as the ratio of the power of the deep muscle contribution to this source to the power of the superficial muscle contribution to this source.

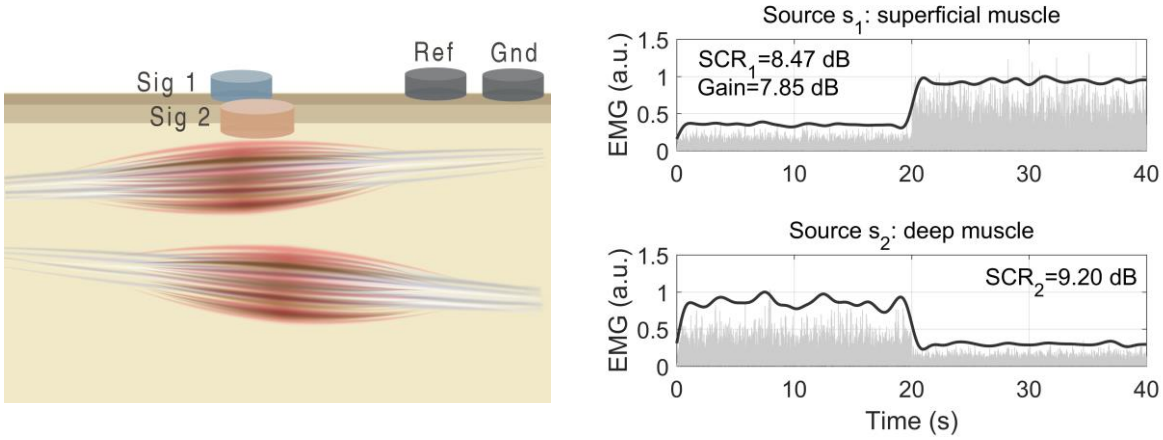

Figure 6. The results of blind source separation application to estimate two sources from the mixtures.

It is seen from the figure that BSS may be used to separate two EMG mixtures into two sources, s_1 and s_2, corresponding to activities of superficial and deep muscles. For superficial muscle, the SCR is 8.47, which is higher than the SCR for double differential method.

MUAP classification algorithm

We recently proposed a peak classification algorithm, which may be also used to reduce a crosstalk from the signals [28]. This algorithm is based on detection of individual peaks in one channel of matrix EMG signal Sig (i,j) (Figure 7), estimating the propagation direction and depth and classifying them in two classes according to active muscle. This method may shows high performance, however, it may fail to separate the mixtures of EMG signals from two muscles active at the same time when the energy of the signal from one muscle is significantly lower than from the second.

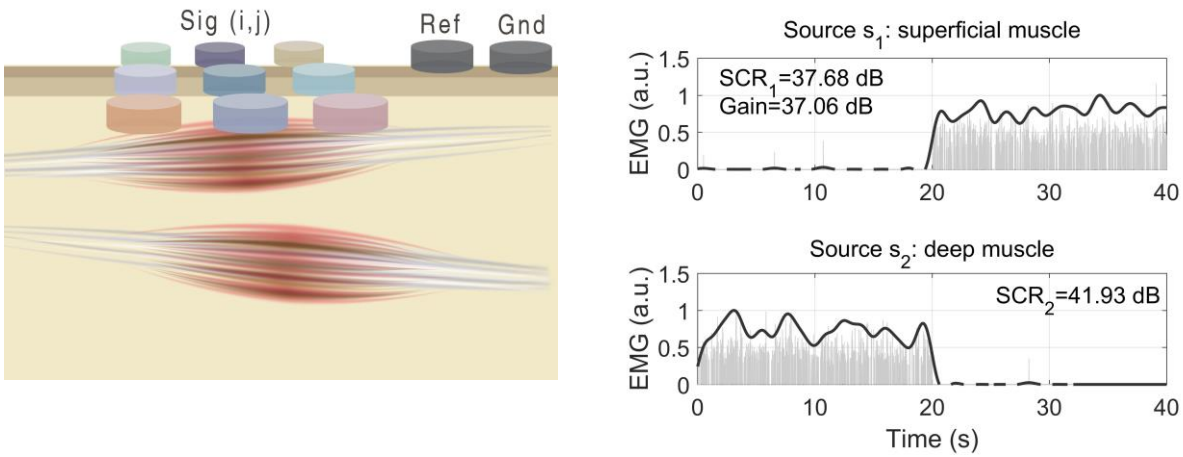

Figure 7. The result of MUP classification algorithm to estimate two sources.

Similarly with BSS, peak classification algorithm may be used to estimate the activities of both sources, superficial and deep muscle.

Descriptive features of EMG signal

Once the EMG signal is preprocessed and separated from the crosstalk, the signal is usually segmented into a series of overlapping on non-overlapping time windows. These windows may be used to calculate some informative characteristics or properties of the signals, characterizing the activity of the muscle of interest and called the descriptive features of the signal. The procedure of passing from signals to a set of estimated features is called the feature extraction. The increase of window size increases the feature estimation performance due to lower variance but reduces the temporal resolution and operation speed for real-time system. In real-time system the window length together with processing time should not be more than 300 ms [29]. For processing time equal to 50 ms the window size may be between 32 and 250 ms [29]. This section firstly presents the feature extraction from single EMG channel and, secondly, presents the feature estimation in case of electrode matrix use.

Feature extraction from single channel EMG

The muscular force is regulated by two main mechanisms: the additional MU recruitment and the increment in the firing rate of MU already actives, both combined in different proportions in diverse muscles. The surface EMG amplitude depends on the same mechanisms, leading to a direct relation between EMG and muscular force estimation, allowing the evaluation of individual muscles contribution to the total force of a synergic group. However, several factors affect the EMG and force relation, such as electrode localization, fiber direction related to acquisition system, subcutaneous tissue, subject variability, session repeatability, and so on. For this reason, is impossible to establish a unique amplitude-force relation. The experimental construction of this relation is even more difficult when the selective activation of a muscular

group is pathological or when other muscles (agonist or antagonist) are involved but is not reflected in a single EMG channel.

Nevertheless, the EMG amplitude remains as a muscular activation estimator and a qualitative index of the change related to a reference condition. In the frequency domain, mean and median power spectral frequencies are been proposed as muscular force estimators, because they reflect the recruitment of new and progressively larger and faster MU, associated to an increment in muscular force. However, spectral characteristics of the EMG are closely related to muscular fatigue and cannot be a reliable estimator of force.

For classification or control purposes, the EMG processing is intended to assign a numeric value to the myolectric level activity, usually associated with MU activation and force, isolating the physiological information for the electric and environmental noise.

A number of studies addresses the question of feature evaluation and selection [30–35]. Below we will present the most relevant and useful features for rehabilitation and biomechanical analysis. In all cases, x_k is the k^{th} sample and N is the sample window size for computation.

- *Integral of Absolute Value (IAV):*

$$IAV = \frac{1}{N}\sum_{k=1}^{N} |x_k| . \quad (5)$$

- *Variance:* the variance is an indicator of the aleatory variable dispersion with reference to the mean value. In signal processing context this feature is used as a power measure of zero-mean signal.

$$VAR = \frac{1}{N-1}\sum_{k=1}^{N} (x_k - \bar{x})^2 . \quad (6)$$

- where $\bar{x}$ is a mean value of EMG signal (expected to be equal to zero).
- *Standard Deviation (STD):* the STD is an indicator of the aleatory variable dispersion with reference to the mean value and expressed the same units as the signal.

$$STD = \sqrt{\frac{1}{N-1}\sum_{k=1}^{N} (x_k - \bar{x})^2} \quad (7)$$

.

- *Root-mean-square* (RMS): root-mean square is a classical power measure of a signal.

$$RMS = \sqrt{\frac{1}{N}\sum_{k=1}^{N} x_k^{\,2}} . \quad (8)$$

- *High-order statistics (HOS):* above-presented features are based on calculating the first and second moments of signal. Higher-order statistics deals with third and higher moments. HOS provide a tool to model non-Gaussian and non-linear signals [36], and can be used in EMG signals as in the work of Nazarpour [37] and Orosco *et al.* [38]. The bispectrum is a third-order

frequency-domain measurement computed as the double Fourier transform of the third-order cumulant sequences, obtaining a complex matrix that needs simplification methods to be used for control or classification purposes. For a detailed explanation see the work of Orosco *et al.* [38].

- *Low pass filtered rectified signal:* the low-pass filtering (below 5 Hz) of the signal is widely used with rectified EMG. Bessel or Butterworth coefficients provide the best response in terms of overshoot and smoothing of the resulting signal.
- *Zero-Cross (ZC)*: zero-cross is a simple frequency measure, which can be obtained counting the number of times that a signal crosses the zero potential line [39]. Given two consecutive data, x_k and x_{k+1} :

$$ZC = \sum_{k=1}^{N} \theta(-x_k \cdot x_{k+1}),$$
$$\theta(x) = \begin{cases} 1 & if\ x > 0 \\ 0 & otherwise \end{cases}, \quad (9)$$

where $\theta(x)$ is a Heaviside function. It is generally applicable to introduce a threshold ε to eliminate zero crossings induced by recording system noise, i.e. take into account only such pairs x_k and x_{k+1} for which a following condition is satisfied:

$$|x_k - x_{k+1}| \geq \varepsilon . \quad (10)$$

The threshold ε depends on recording system noise.

- *Waveform Length (WL):* This feature provides information about signal complexity in each window [39]. The resulting value combine amplitude, frequency and duration in a single feature, simply computing the cumulative length of the signal in the window:

$$WL = \sum_{k=1}^{N} |\Delta x_k|,$$
$$\Delta x_k = x_k - x_{k-1}. \quad (11)$$

- *Willison Amplitude (WAMP):* WAMP [40] indicates the count number for each change in the EMG amplitude that exceeds a predefined threshold ε. It reflects the action potential firing of MUs and therefore the level of contraction [31,35].

$$WAMP = \sum_{k=1}^{N} f\left(|x_k - x_{k+1}|\right),$$
$$f(n) = \begin{cases} 1 & if\ n > \varepsilon \\ 0 & otherwise \end{cases}. \quad (12)$$

- *Time series modelling:* A stationary Gaussian stochastic signal can be modeled as an autoregressive linear time series (AR), as in the classical approach by Box and Jenkins [41].

$$x_k = \sum_{i=1}^{p} a_i x_{k-i} + e_k \,, \qquad (13)$$

where a_i represents the AR coefficients, p the order of the model and e_k the residual noise. Since the spectrum of the signal changes with the contractile state of the muscle it is possible to estimate it by monitoring the AR or ARMA coefficients [42]. This consideration is not strictly correct because this model involves stationary signals, but it can be done in data windows to overcome this inconvenience. So, it is possible to segment the areas where resting phases alternate with contraction phases, and then make the model identification toolbox using an ARMA model. In bibliography, it was found that polynomials of 8th order or higher provide a good representation of the signal

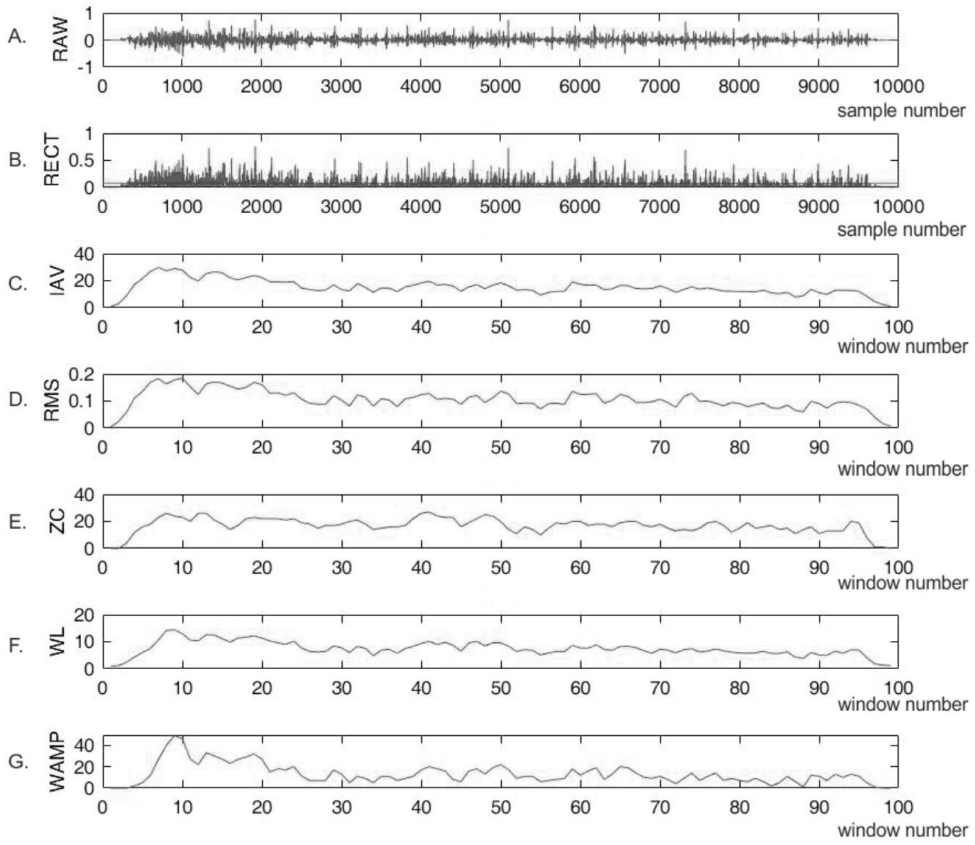

Figure 8. Temporal Domain Features extracted from a typical EMG signal: IAV, RMS, ZC, WL, WAMP. (A) Raw EMG signal (Sample Frequency of 1 kHz), samples in x axis. (B) Rectified signal and mean value (red line). C to G Figures show temporal features performed in windows of 200 samples with an overlap of 100 samples. In this case, x axis indicates the window number. (C) IAV (D) RMS (E) ZC (F) WL (G) WAMP.

Feature extraction from matrix EMG

The signal from an electrode of the electrode matrix may be used to estimate the features in temporal domain, presented above. Moreover, using the electrode matrix or array gives an information about the muscle contour or active region (spatial features), the velocity and direction of activation propagation within a muscle, the depth of muscular activity, and location

of muscle innervation zones. Jordanic *et al*. [43] demonstrated that using special features can improve performance of muscular activity classification on patients with incomplete spinal cord injury. Below we present an example of two spatial features. Rojas-Martinez *et al.* [44] used the coordinates of the center of gravity **CG** and maximal intensity **MX** of the active region under the matrix to distinguish among the different motor tasks. The *x* and *y* components of **CG** are**:**

$$CG_x = \frac{\sum_{i=1}^{N_r}\sum_{j=1}^{N_c} RMS(i,j)\cdot x(i,j)}{\sum_{i=1}^{N_r}\sum_{j=1}^{N_c} RMS(i,j)}, \qquad (14)$$

$$CG_y = \frac{\sum_{i}^{N_r}\sum_{j}^{N_c} RMS(i,j)\cdot y(i,j)}{\sum_{i}^{N_r}\sum_{j}^{N_c} RMS(i,j)}$$

where $RMS(i,j)$ is a root mean square value of EMG calculated for the electrode located in i-*t*h row and *j*-th column of the matrix, N_r and N_c are the number of electrodes in one row and one column of matrix. The values $x(i,j)$ and $y(i,j)$ are x and y coordinates of the electrode, located in i-*t*h row and *j*-th column of the matrix.

The components of **MX** are**:**

$$\begin{aligned} MX_x &= x(i_{\max}, j_{\max}) \\ MX_y &= y(i_{\max}, j_{\max}) \\ RMS(i_{\max}, j_{\max}) &= \max \end{aligned}, \qquad (15)$$

where i_{max} and j_{max} are the numbers of electrode row and column for which the RMS value is maximal in given temporal sample window.

Moreover, EMG matrix signals may be used to extract individual MUAP trains and identify the features of each MUAP train separately. The number of MU to be separately identified depends on muscle activation level. The state-of art decomposition technics allows identifying up to 20 MUAP for moderate muscle activation level [45].

The practical use of EMG signal

The use of EMG in biomechanical studies

The EMG signal is widely used in biomechanics as an indicator of muscle force. Previously presented features (low-pass filtered rectified signal, RMS, IAV) are related with muscle activation level. Biomechanics is interested in estimating the force, performed by muscle

and expressed in Newtons (N). Therefore, biomechanics aims at transforming the features of EMG signal into a force value. In previous sections, we represented the EMG signals as functions of discrete sample number *k.* Below we assume that both the force and the EMG envelope are functions of continues time *t* for simplicity. One should also notice the EMG-force relationships, presented below, may be accepted only for isometric tasks. In dynamics tasks, muscle force must be considered as a function of muscle state (fiber elongation and contraction velocity). Below we also neglect an electromechanical delay between the variation of EMG and force.

Direct force estimation from single-channel EMG

There is a monotonic relationship between the envelope of EMG and force of muscle $F(t)$. To obtain signal envelope one can use, for example, the low-pass filtered rectified signal, RMS, or IAV. This relationship depends on anatomical and detection conditions. The simplest relationship is a linear one, which is widely used [1,46]:

$$F(t) = \alpha \hat{x}(t), \quad (16)$$

where α is a parameter of the model and $\hat{x}(t)$ is a normalized envelope of the EMG signal $x(t)$. The envelope is normalized by its peak value, attained when a subject performs a maximum voluntary contraction (MVC). In this case, a parameter α corresponds to the force, attained by a muscle during MVC. This coefficient may be related with physiological cross-sectional area of the muscle as

$$\alpha = \sigma_{\max} \cdot PCSA, \quad (17)$$

where $\sigma_{\max}$ is a maximal force, which may be produced by a muscle section with unitary PSCA (maximum muscle stress, specific tension). For example, Chao *et al.* [47] reports PCSA equal to 1.5±0.6 cm^2 for *abductor pollicis brevis muscle* and 10.0±3.0 cm^2 for *flexor capri ulnaris* muscle. A maximum muscle stress was reported to be 35 N/cm^2 by Zajac *et al.* [48].

A nonlinear model between EMG and force was used by Potvin *et al.* [49] and Lloyd *et al.* [50]

$$F(t) = \beta \frac{e^{-\alpha \hat{x}(t)} - 1}{e^{-\alpha} - 1}, \quad (18)$$

where α and β are the parameters of the model.

Direct force estimation from matrix EMG

One can benefit from using matrix EMG signal, which cover the large surface of the muscle and provides the distribution of the potential over its surface to make a more precise estimation of muscle force. Staudenmann *et al*. [51,52] studied improvement of muscle force estimation precision in case of using a matrix of electrodes, compared to single-channel EMG recording. In [51], the authors rectified the signals from a number of HD-EMG matrix channels, averaged them, and applied low-pass filtering to estimate the force from HD-EMG recording. They reported 30% improvement of muscle force estimation precision compared to single-channel EMG recording. In [52], the authors firstly applied principal component analysis to transform the signals from HD-EMG matrix into a set of principle modes. Next, they chose an optimal combination of principal modes, rectified this combination, and applied low-pass filtering. In case of using PCA the authors reported 40% improvement of muscle force estimation precision compared to single-channel EMG recording.

Force estimation by a biomechanical model assisted by EMG

If one aims in estimating a force of a muscle, actuating the extremity, using the EMG signal is not the only way to do it. The unknown muscle force is related with the force produced by an extremity. If the extremity is fixed (*i.e.* a static isometric problem), the force produced by it may be measured directly. Therefore, an unknown muscle force may be calculated from the measured extremity force by means of a biomechanical model. However, it is difficult to find a case, in which the extremity force is produced by action of only one muscle. In most cases, it is a result of multiple muscle activations. For example, the force of a middle finger tip, applied to a keyboard button when typing a text, is produced by activation of six muscles, *flexor digitorum profundus*, *flexor digitorum superficialis*, two *interosseus*, *lumbriacal and extensor digitiorum communis.* The last muscle is an antagonist for flexor muscles; however, it can be involved in this pushing action (muscle coactivation phenomenon). Therefore, the problem becomes the following: one have to estimate a set of muscle forces, which produces a known force and torque at the end of extremity. It is an ill-posed problem, which may have an infinite number of solutions. One of the promising possibilities to find an appropriate set of muscle forces is to use a biomechanical model assisted by EMG. There are a lot of different variations of this approach. One method of muscle force set estimation was proposed by Vigouroux *et al.* [53] for an extremity, fixed in static conditions. The method is based on the following idea. One must solve an optimization problem and to find such a set of muscle forces $F_i(t)$, which minimizes some physiological cost-function, which may be an overall stress in active muscles. In this case, *i*

represents an index number of a muscle in a set. The solution must satisfy two conditions. Firstly, the solution must satisfy the biomechanical equilibrium equations. Secondly, for each i^{th} muscle, for which the EMG signal $x_i(t)$ is measured, the estimated force $F_i(t)$ must not deviate from the value, estimated with the help of one direct EMG-force models, e.g. (16), more than for a predefined threshold ε:

$$\left|F_i(t) - \alpha \hat{x}_i(t)\right| \le \varepsilon . \quad (19)$$

Therefore, this method combines the information from the EMG electrodes, measured from several muscles, and the force measured from the end of extremity to estimate the forces in all muscles, actuating the extremity. The threshold ε depends on quality of EMG signal recording, including the quantity of crosstalk. The better the signal quality is, the less the threshold ε may be. The EMG-assisted force estimation may be a powerful method when estimating the forces from deep muscles, which may difficult to characterize by direct EMG-force modeling.

In this paragraph, we presented different techniques of muscle force estimation based on EMG signal. Whatever technique is chosen, the muscle force estimation precision depends on quality of EMG signals, including the crosstalk quantity. For example, if the single-channel EMG recording from a muscle is perturbed by a crosstalk from a nearby muscle active at the same time, such as the power of crosstalk is 25% of the signal power of EMG from the muscle of interest (SCR of 6 dB), using a linear relationship (14) to estimate a force in a muscle of interest will lead to a force estimation error of 12%[2]. Therefore, an attention must be paid to EMG signal quality prior to force estimation.

[2] In this example we assume that EMG of muscle of interest and crosstalk are independent processes and that the standard deviation of EMG of muscle of interest is equal to σ_1 and the standard deviation of crosstalk is equal to $\sigma_2 = 0.5\sigma_1$, which corresponds to 25% of muscle of interest EMG power. Therefore, the standard deviation of the sum of the muscle of interest EMG and crosstalk is equal to $\sigma_3 = \sqrt{\sigma_1^2 + \sigma_2^2} \approx 1.12 \cdot \sigma_1$, which is 12% higher than the standard deviation of muscle of interest EMG. If the linear relationship between the force and root-mean square value of EMG signal is used, it will lead to a force estimation error of 12%.

The use of EMG in Muscle Coordination Analysis

Human movement and behavior are the result of complex dynamics between the nervous system, proprioceptive receptors and muscles. The Central Nervous System (CNS) is able to choose between several possible options when performing a motor task due to the redundancy of the musculoskeletal system [54]. In this context the concept of Muscular Synergy (MS) appears, whose usefulness is determined by its ability to faithfully describe patterns of muscle activation using fewer dimensions than the number of registered muscles [55]. However, it is still a research topic how the SNC combines these modules in different ways to perform specific tasks.

The concept of Muscle Synergy in EMG was introduced approximately two decades ago [56] and has gained popularity in recent years. In a simple way, a MS is defined as a group of muscles that are activated in a coordinated way during the execution of a motor task. In the spatial domain (between muscles), MS captures the specific relationship in muscle activation amplitudes. Considering a set of *d* muscles, a MS can be expressed as a *d*-dimensional vector **w** of weighting coefficients that specify the balance of activation between the muscles [57]. Different levels of activation can be generated by a single muscular synergy by scaling the entire vector in amplitude:

$$\mathbf{m} = c\mathbf{w}, \quad (20)$$

where **m** is a vector that specifies a muscle activation pattern given by the level of recruitment of each muscle and by a scale coefficient *c*. More generally, a set of *N* synergies $\{\mathbf{w}_i\}$, $i = 1 \ldots N$, can generate many different muscle patterns by linear combination:

$$\mathbf{m} = c_1\mathbf{w}_1 + c_2\mathbf{w}_2 + \ldots + c_N\mathbf{w}_N = \sum_{i=1}^{N} c_i\mathbf{w}_i, \quad (21)$$

where c_i is the scaling coefficient for the i^{th} synergy.

Since the muscle activation vectors involved in most behaviors depend on time, relationships between muscles synergies can also be found in the temporal domain. With respect to time, a synergy can be invariant or variant over time. A synergy is invariant over time if the same muscle activation balance, expressed by a vector *w*, is maintained at all times, that is, for all activation vectors that vary over time and that comprise muscle patterns (the muscles are activate in sync with fixed weights). If all synergies are invariant over time, then:

$$\mathbf{m}(t) = \sum_{i=1}^{N} c_i(t)\mathbf{w}_i, \quad (22)$$

where $\mathbf{m}(t)$ is muscle activation vector at time t and $c_i(t)$ is the scale coefficient for the i^{th} synergy at time t. Since each invariable synergy over time contributes to the waveform of different muscles with the same $c_i(t)$ waveform, the muscle waveforms associated with each synergy are synchronous. In contrast, a time-varying synergy is composed of a collection of waveforms, each specific to a muscle, and therefore not necessarily synchronous. These waveforms can be expressed by a time-varying synergy vector $\mathbf{w}(t)$ that can be written with a scale coefficient c_i and a time delay t_i for each synergy:

$$\mathbf{m}(t) = \sum_{i=1}^{N} c_i \mathbf{w}(t - t_i). \quad (23)$$

In this case, the temporal dependence of the muscle activation waveforms is captured by the temporal structure of the synergies and their relative delays. Variable synergies over time represent motor output because, once synergies occur, a few scale and delay coefficients are sufficient to specify many muscle patterns. Muscular synergy constitutes the coordinated activation of muscle groups with fixed profiles that vary over time.

Research suggests that the CNS produces different movements by controlling the muscles through the flexible combination of these synergies [58]. The MS acquire the role of movement building blocks that define characteristic activation patterns for each individual, which has a great implication in the understanding of the organization and structure of the CNS, and gives a way through which motor intentions at the level of a task are translated into low-level muscle activation patterns. Many studies analyze EMG data through correlational and computational methods in order to see if muscle synergies exist and if these synergies are relevant to the task [59–61].

A proposed analysis method combines the quantification of kinematics and electromyographic evaluation. For example, in [62] it is interpreted that different neuromuscular synergies are involved in the execution of the movement and it is hypothesized that the feedforward motor commands involved in trajectory planning are different. Muceli *et al.* [63] investigate the possibility of describing a task by a linear combination of a set of MS common to multiple directions through the surface EMG record. The registration of surface electromyographic signals of 12 muscles of the upper limb is performed for different proposed movements involved both one and several joints and were generated in 12 directions of the horizontal plane. Motion kinematics was recorded using a motion analysis system. Muscular synergies were extracted, the results of which indicate that a large set of multiarticular

movements can be generated by a synergistic matrix of limited dimensionality and common to all directions if synergies are extracted from a representative number of directions.

A recent work proposes the use of techniques such as coherence and causality to obtain MS in order to associate them with the generation of a given movement [61]. Coherence analysis was used to evaluate the relation of two sets of EMG signals in the frequency domain. The coherence spectra is defined as the magnitude squared of the cross spectrum, normalized by the product of the auto spectra of the two individual data sets [60]. Equation (24) shows the formula for coherence between two signals, *x(t)* and *y(t)*.

$$C_{xy}(f) = \frac{\left|G_{xy}(f)\right|^2}{G_{xx}(f).G_{yy}(f)}. \quad (24)$$

where G_{xy} is the cross-spectral density between *x(t)* and *y(t)*. G_{xx} and G_{yy} are the autospectral density of *x* and *y* respectively.

Coherence analysis provides an information about the degree of linear dependency between *x* and *y* for different frequencies *f* of the signals. For each frequency, $C_{xy}(f)$ has the value between 0 (no dependency) and 1 (perfect dependency).

Wiener-Granger Causality (GC) is a popular method used in econometrics and allows to identifying "causal" connectivity between signals. Let $x(t)$ and $y(t)$ be two signals taken from two data channels. Suppose that the temporal dynamics of $x(t)$ and $y(t)$ are suitably represented by the following bivariate autoregressive process:

$$\begin{aligned} x(t) &= \sum_{j=1}^{p} a_{11}(j)x(t-j) + \sum_{j=1}^{p} a_{12}(j)y(t-j) + e_1, \\ y(t) &= \sum_{j=1}^{p} a_{21}(j)x(t-j) + \sum_{j=1}^{p} a_{22}(j)y(t-j) + e_2. \end{aligned} \quad (25)$$

Here a_{11}, a_{12}, a_{21}, a_{22} represent regression coefficients; e_1, e_2 represent the regression residuals and p the time lags. A variable *x* "G-Cause" a variable *y* if the past of *x* contains information that helps predict the future of *y* over and above information already in the past of *y*. The method provides a statistical description of observed responses. Computation of G-causality requires specification of the regression model order. Two suitable criteria are the Akaike information criterion [64] and the Bayesian information criterion [65–67]. The figure below was modified from [61] and shows a graphic representation of GC connections found during a wrist

flexion movement. Here the numbers 1, 2, 3 represent the EMG signals recorded from electrodes placed on three different muscles (*flexor carpi radialis, brachioradialis, flexor carpi ulnaris respectively*).

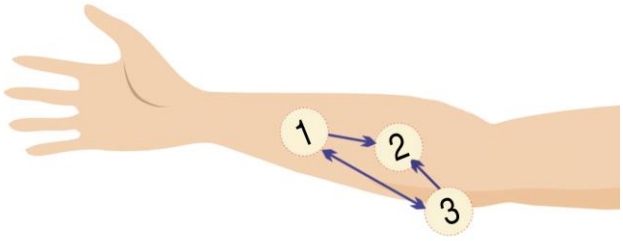

Figure 9. GC connections during a Wrist Flexion Motion. Numbers represent the EMG signals recorded from electrodes placed on different muscles. The graph shows causal relationships between channels 1 (flexor carpi radialis), 2 (brachioradialis) and 3 (flexor carpi ulnaris).

The use of EMG in myoelectric control

As was pointed out in this chapter, electromyographic signal has a wide range of applications, in biomechanics, diagnoses, sensorimotor integration, prostheses control, and rehabilitation. The information extracted for the EMG can provide a useful tool for quantitative measurement and analysis of conduction velocity, motor unit recruitment, synergies, muscular force and tone, and other physiological variables, as well as control signal for rehabilitation devices.

Restoration and assessment of motor function is the main objective of neurorehabilitation, in which technological and robotic systems can produce an important breakthrough in clinical practice. This is especially important in post stroke patients, when cerebral lesions change motor control ability of the CNS to perform voluntary movements, leading to inadequate planification and muscular co-contraction. In this case, the EMG (sometimes combined with brain evaluation trough images or electroencephalographic signals) appears as a method to estimate the motor plan reorganization and establish, redefine or modify a personalized rehabilitation therapy.

In terms of myoelectric control, it is possible to establish a simple scheme to represent the main parts of any assistive device driven by EMG signal, as is pointed out in Figure 10.

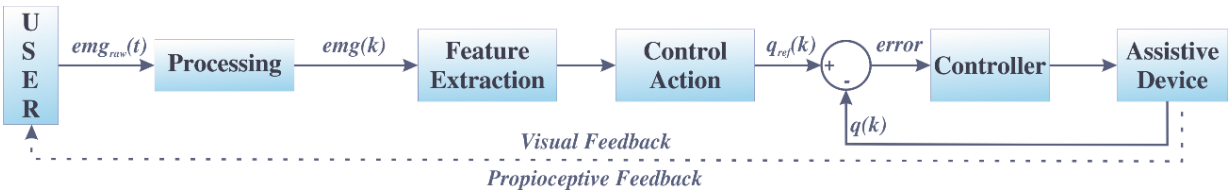

Figure 10. Flowchart describing a classical scheme of myoelectric control. The Processing stage correspond to signal conditioning, filters and windowing, obtaining emg(k) as the myoelectric signal in each k sampled time. The muscle contraction amplitude is estimated in Feature Extraction block and transformed in a control action, i.e. a reference qref(k) for the assistive device. Control feedback is performed through internal sensors to obtain q(k). The user feedback has two main components: Visual and proprioceptive. (Modified from [68]*)*

The natural control that a person wields on his musculoskeletal system depends on a closed loop system comprising the generation of command motor signals from the central nervous system (CNS) used in the direct loop and feedback by sensory signals from proprioceptive receptors muscle and vision (Figure 10). An ideal robotic assistance system should provide an interface with the remaining neuromuscular system as close to the physiological as possible. In this context there are still many limitations both in the motor loop and in the sensory (tactile) and proprioceptive feedback.

The myoelectric control can be implemented with one or two channels, since in the latter case two sites of muscular activity are sensed and the channel with the highest level is chosen [68]. In addition, once the operating state is selected, the device can be activated (ON/OFF control) or determined by the level of myoelectric activity (proportional control).

The best performance of the system is obtained when the affected muscles are commanded in the same way as they were used before the neuromotor lesion or disease, because the patient retains a cortical image of the movement and is able to repeat a complex pattern of muscle activation to get it.

However, the result depends on the type of device control strategies and user training. In general, low acceptance rates of success occur when the patient perceives inadequate controllability, a gap between intuitive and expert control. The control problem is more complex and has led to the development of new and better techniques for statistical signal processing and classifiers to extract more information from the signal. In recent decades, significant progress has occurred both in the optimization and miniaturization of associated electronics and mechanics; as in the development of new and better processing techniques, classification through neural networks, reinforcement learning, and so on.

Achieving user motivation during rehabilitation is an important concern. Different strategies have been analyzed to improve patient adhesion during robot-assisted rehabilitation [70]. The collaborative use of EMG and haptic or virtual reality devices can improve the

subject's participation in rehabilitation. Yoo *et al*. [71] analyze the effect of using Virtual Reality (VR) games and EMG feedback on neuromotor control in patients with cerebral palsy. Van de Meent *et al.* [71] evaluate the potential use of VR and EMG in a rehabilitation device for critical diseases. On the other hand, devices that combine EMG signals with haptic feedback have also had a great development and their effect has been studied in several works [73,74]. Myoelectric gaming appears as a good proposal to improve the rehabilitation process of patients with different pathological conditions [75].

References

[1] J. V Basmajian, C.J. de Luca, Muscles Alive : their functions revealed by electromyography, Williams & Wilkins, Baltimore, 1985.

[2] E. (Novato I. for S.R. and T. Criswell, ed., Cram's Introduction to Surface Electromyography, 2nd ed., Jones and Bartlett Publishers, 2011.

[3] R. Merletti, P.A. Parker, Electromyography. Physiology, Engineering, and Noninvasive Applications, 2004. doi:10.1002/0471678384.

[4] R. Merletti, D. Farina, eds., Surface Electromyography : Physiology, Engineering, and Applications, John Wiley & Sons, Inc., Hoboken, New Jersey, 2016. doi:10.1002/9781119082934.

[5] C.J. de Luca, The use of surface electromyography in biomechanics, J. Appl. Biomech. 13 (1997) 135–163. doi:citeulike-article-id:2515246.

[6] H.J. Hermens, B. Freriks, R. Merletti, D. Stegeman, J. Block, G. Rau, C. Disselhorst-Klug, G. Hagg, SENIAM European Recomendation for Surface Electromyography, 8th ed., Roessingh Research and Development b.v., 1999.

[7] M. Besomi, P.W. Hodges, J. Van Dieën, R.G. Carson, E.A. Clancy, C. Disselhorst-Klug, A. Holobar, F. Hug, M.C. Kiernan, M. Lowery, K. McGill, R. Merletti, E. Perreault, K. Søgaard, K. Tucker, T. Besier, R. Enoka, D. Falla, D. Farina, S. Gandevia, J.C. Rothwell, B. Vicenzino, T. Wrigley, Consensus for experimental design in electromyography (CEDE) project: Electrode selection matrix, J. Electromyogr. Kinesiol. 48 (2019) 128–144. doi:10.1016/j.jelekin.2019.07.008.

[8] D. Noble, Applications of Hodgkin-Huxley equations to excitable tissues., Physiol. Rev. 46 (1966) 1–50. doi:10.1152/physrev.1966.46.1.1.

[9] P. Rosenfalck, Intra- and extracellular potential fields of active nerve and muscle fibres. A physico-mathematical analysis of different models., Acta Physiol. Scand. Suppl. 321

(1969) 1–168. http://www.physiology.org/doi/10.1152/physrev.1966.46.1.1.

[10] B. Afsharipour, S. Soedirdjo, R. Merletti, Two-dimensional surface EMG: The effects of electrode size, interelectrode distance and image truncation, Biomed. Signal Process. Control. 49 (2019) 298–307. doi:10.1016/j.bspc.2018.12.001.

[11] D. Farina, R. Merletti, A novel approach for precise simulation of the EMG signal detected by surface electrodes, IEEE Trans. Biomed. Eng. 48 (2001) 637–646. doi:10.1109/10.923782.

[12] L. Mesin, Optimal spatio-temporal filter for the reduction of crosstalk in surface electromyogram, J. Neural Eng. 15 (2018) 016013. doi:10.1088/1741-2552/aa8f03.

[13] D. Farina, C. Févotte, C. Doncarli, R. Merletti, Blind Separation of Linear Instantaneous Mixtures of Nonstationary Surface Myoelectric Signals, IEEE Trans. Biomed. Eng. 51 (2004) 1555–1567.

[14] M. Léouffre, F. Quaine, C. Servière, Testing of instantaneity hypothesis for blind source separation of extensor indicis and extensor digiti minimi surface electromyograms., J. Electromyogr. Kinesiol. 23 (2013) 908–15. doi:10.1016/j.jelekin.2013.03.009.

[15] R. Merletti, A. Holobar, D. Farina, Analysis of motor units with high-density surface electromyography., J. Electromyogr. Kinesiol. 18 (2008) 879–90. doi:10.1016/j.jelekin.2008.09.002.

[16] P. Comon, Independent component analysis, A new concept?, Signal Processing. 36 (1994) 287–314. doi:10.1016/0165-1684(94)90029-9.

[17] F. Negro, S. Muceli, A.M. Castronovo, A. Holobar, D. Farina, Multi-channel intramuscular and surface EMG decomposition by convolutive blind source separation, J. Neural Eng. 13 (2016) 026027. doi:10.1088/1741-2560/13/2/026027.

[18] A. Belouchrani, K. Abed-Meraim, J.-F. Cardoso, E. Moulines, A blind source separation technique using second-order statistics, IEEE Trans. Signal Process. 45 (1997) 434–444. doi:10.1109/78.554307.

[19] G.R. Naik, S.E. Selvan, M. Gobbo, A. Acharyya, H.T. Nguyen, Principal Component Analysis Applied to Surface Electromyography: A Comprehensive Review, IEEE Access. 4 (2016) 4025–4037. doi:10.1109/ACCESS.2016.2593013.

[20] G. Bosco, Principal Component Analysis of Electromyographic Signals: An Overview, Open Rehabil. J. 3 (2010) 127–131. doi:10.2174/1874943701003010127.

[21] A.J. Bell, T.J. Sejnowski, An information-maximization approach to blind separation and blind deconvolution., Neural Comput. 7 (1995) 1129–59. doi:doi:10.1162/neco.1995.7.6.1129.

[22] A. Hyvarinen, Fast and robust fixed-point algorithms for independent component analysis, IEEE Trans. Neural Networks. 10 (1999) 626–634. doi:10.1109/72.761722.

[23] J. Cardoso, A. Souloumiac, Blind beamforming for non-Gaussian signals, IEE Proc. F (Radar Signal Process. 140 (1993) 362–370. http://digital-library.theiet.org/content/journals/10.1049/ip-f-2.1993.0054 (accessed December 17, 2014).

[24] D. Pham, J.-F. Cardoso, Blind separation of instantaneous mixtures of nonstationary sources, IEEE Trans. Signal Process. 49 (2001) 1837–1848. doi:10.1109/78.942614.

[25] G.R. Naik, A comparison of ICA algorithms in surface EMG signal processing, Int. J. Biomed. Eng. Technol. 6 (2011) 363. doi:10.1504/IJBET.2011.041774.

[26] N. Jiang, D. Farina, Covariance and time-scale methods for blind separation of delayed sources, IEEE Trans. Biomed. Eng. 58 (2011) 550–556. doi:10.1109/TBME.2010.2084999.

[27] D. Pham, C. Serviere, H. Boumaraf, Blind separation of convolutive audio mixtures using nonstationarity, Proceeding ICA 2003 Conf. (2003) pp. 975–980. http://bsp.teithe.gr/members/downloads/bssaudio/references/sepa-audioR.pdf.

[28] A. Dogadov, C. Serviere, F. Quaine, Extraction of EI and EDM muscle sources from surface electromyographic signals using delay estimation, in: BioSMART, IEEE, Dubai, 2016: p. 4. doi:10.1109/BIOSMART.2016.7835471.

[29] M.A. Oskoei, H. Hu, Myoelectric control systems — A survey, 2 (2007) 275–294. doi:10.1016/j.bspc.2007.07.009.

[30] D. Tkach, H. Huang, T.A. Kuiken, Study of stability of time-domain features for electromyographic pattern recognition, J. Neuroeng. Rehabil. 7 (2010) 1–13. doi:10.1186/1743-0003-7-21.

[31] M. Zardoshti-Kermani, B.C. Wheeler, K. Badie, R.M. Hashemi, EMG feature evaluation for movement control of upper extremity prostheses, IEEE Trans. Rehabil. Eng. 3 (1995) 324–333. doi:10.1109/86.481972.

[32] M.A. Oskoei, H. Hu, GA-based Feature Subset Selection for Myoelectric Classification,

in: 2006 IEEE Int. Conf. Robot. Biomimetics, IEEE, 2006: pp. 1465–1470. doi:10.1109/ROBIO.2006.340145.

[33] A. Phinyomark, P. Phukpattaranont, C. Limsakul, Feature reduction and selection for EMG signal classification, Expert Syst. Appl. 39 (2012) 7420–7431. doi:10.1016/j.eswa.2012.01.102.

[34] A. Phinyomark, R.N. Khushaba, E. Scheme, Feature extraction and selection for myoelectric control based on wearable EMG sensors, Sensors (Switzerland). 18 (2018) 1–17. doi:10.3390/s18051615.

[35] E. Scheme, K. Englehart, On the robustness of EMG features for pattern recognition based myoelectric control; A multi-dataset comparison, in: 2014 36th Annu. Int. Conf. IEEE Eng. Med. Biol. Soc., IEEE, 2014: pp. 650–653. doi:10.1109/EMBC.2014.6943675.

[36] C.L. Nikias, J.M. Mendel, Signal processing with higher-order spectra, IEEE Signal Process. Mag. 10 (1993) 10–37. doi:10.1109/79.221324.

[37] K. Nazarpour, A. Barnard, A. Jackson, Flexible Cortical Control of Task-Specific Muscle Synergies, J. Neurosci. 32 (2012) 12349–12360. doi:10.1523/JNEUROSCI.5481-11.2012.

[38] E.C. Orosco, N.M. Lopez, F. Di Sciascio, Bispectrum-based features classification for myoelectric control, Biomed. Signal Process. Control. (2013). doi:10.1016/j.bspc.2012.08.008.

[39] B. Hudgins, P. Parker, R.N. Scott, A New Strategy for Multifunction Myoelectric Control, IEEE Trans. Biomed. Eng. 40 (1993) 82–94. doi:10.1109/10.204774.

[40] R.G. Willison, A method for measuring motor unit activity in human muscle, J. Physiol. 168 (1963) 29–41. doi:10.1113/jphysiol.1963.sp007235.

[41] G.E.P. Box, G.M. Jenkins, Time series analysis: forecasting and controle, Holden-Day, San Francisco, 1970.

[42] D. Graupe, J. Salahi, D. Zhang, Stochastic analysis of myoelectric temporal signatures for multifunctional single-site activation of prostheses and orthoses, J. Biomed. Eng. 7 (1985) 18–29. doi:10.1016/0141-5425(85)90004-4.

[43] M. Jordanic, M. Rojas-Martínez, M.A. Mañanas, J.F. Alonso, Spatial distribution of HD-EMG improves identification of task and force in patients with incomplete spinal cord injury, J. Neuroeng. Rehabil. 13 (2016) 1–11. doi:10.1186/s12984-016-0151-8.

[44] M. Rojas-martínez, M.A. Mañanas, J.F. Alonso, R. Merletti, Identification of isometric contractions based on High Density EMG maps, J. Electromyogr. Kinesiol. 23 (2013) 33–42. doi:10.1016/j.jelekin.2012.06.009.

[45] E. Stålberg, H. Van Dijk, B. Falck, J. Kimura, C. Neuwirth, M. Pitt, S. Podnar, D.I. Rubin, S. Rutkove, D.B. Sanders, M. Sonoo, H. Tankisi, M. Zwarts, Clinical Neurophysiology Standards for quantification of EMG and neurography, 130 (2019) 1688–1729. doi:10.1016/j.clinph.2019.05.008.

[46] O.C.J. Lippold, The relation between integrated action potentials in a human muscle and its isometric tension, J. Physiol. 117 (1952) 492–499.

[47] E.Y. Chao, Biomechanics of the Hand: A Basic Research Study, World Scientific, 1989. https://books.google.fr/books?id=7SI5NJDC5gIC.

[48] F.E. Zajac, Muscle and tendon: properties, models, scaling, and application to biomechanics and motor control., Crit. Rev. Biomed. Eng. 17 (1989) 359–411.

[49] J.R. Potvin, R.W. Norman, S.M. McGill, Mechanically corrected EMG for the continuous estimation of erector spinae muscle loading during repetitive lifting, Eur. J. Appl. Physiol. Occup. Physiol. 74 (1996) 119–132. doi:10.1007/BF00376504.

[50] D.G. Lloyd, D.G. Lloyd, T.F. Besier, An EMG-driven musculoskeletal model to estimate muscle forces and knee joint moments in vivo An EMG-driven musculoskeletal model to estimate muscle forces and knee joint moments in vivo, (2003). doi:10.1016/S0021-9290(03)00010-1.

[51] D. Staudenmann, I. Kingma, D.F. Stegeman, J.H. Van Diee, Towards optimal multi-channel EMG electrode configurations in muscle force estimation : a high density EMG study, J. Electromyogr. Kinesiol. 15 (2005) 1–11. doi:10.1016/j.jelekin.2004.06.008.

[52] D. Staudenmann, I. Kingma, A. Daffertshofer, D.F. Stegeman, J.H. Van Dieën, Improving EMG-based muscle force estimation by using a high-density EMG grid and principal component analysis, IEEE Trans. Biomed. Eng. 53 (2006) 712–719. doi:10.1109/TBME.2006.870246.

[53] L. Vigouroux, F. Quaine, A. Labarre-Vila, D. Amarantini, F. Moutet, Using EMG data to constrain optimization procedure improves finger tendon tension estimations during static fingertip force production, J. Biomech. 40 (2007) 2846–2856. doi:10.1016/j.jbiomech.2007.03.010.

[54] F. Alnajjar, T. Wojtara, H. Kimura, S. Shimoda, Muscle synergy space: learning model to create an optimal muscle synergy, Front. Comput. Neurosci. 7 (2013). doi:10.3389/fncom.2013.00136.

[55] A. d'Avella, A. Portone, L. Fernandez, F. Lacquaniti, Control of Fast-Reaching Movements by Muscle Synergy Combinations, J. Neurosci. 26 (2006) 7791–7810. doi:10.1523/JNEUROSCI.0830-06.2006.

[56] M. Flanders, U. Herrmann, Two components of muscle activation: scaling with the speed of arm movement, J. Neurophysiol. 67 (1992) 931–943. doi:10.1152/jn.1992.67.4.931.

[57] L.H. Ting, J.L. McKay, Neuromechanics of muscle synergies for posture and movement, Curr. Opin. Neurobiol. 17 (2007) 622–628. doi:10.1016/j.conb.2008.01.002.

[58] M.C. Tresch, A. Jarc, The case for and against muscle synergies, Curr. Opin. Neurobiol. 19 (2009) 601–607. doi:10.1016/j.conb.2009.09.002.

[59] T.W. Boonstra, M. Breakspear, Neural mechanisms of intermuscular coherence: implications for the rectification of surface electromyography, J. Neurophysiol. 107 (2012) 796–807. doi:10.1152/jn.00066.2011.

[60] A. Danna-Dos Santos, B. Poston, M. Jesunathadas, L.R. Bobich, T.M. Hamm, M. Santello, Influence of Fatigue on Hand Muscle Coordination and EMG-EMG Coherence During Three-Digit Grasping, J. Neurophysiol. 104 (2010) 3576–3587. doi:10.1152/jn.00583.2010.

[61] F.J. Muñoz Z., N.M. López C., F. Roberti, M.E. Valentinuzzi, Muscle Synergies for Motor Control Evaluation BT - World Congress on Medical Physics and Biomedical Engineering 2018, in: L. Lhotska, L. Sukupova, I. Lacković, G.S. Ibbott (Eds.), Springer Singapore, Singapore, 2019: pp. 529–533.

[62] A.M. Sabatini, Identification of neuromuscular synergies in natural upper-arm movements, Biol. Cybern. 86 (2002) 253–262. doi:10.1007/s00422-001-0297-7.

[63] S. Muceli, A.T. Boye, A. D'Avella, D. Farina, Identifying Representative Synergy Matrices for Describing Muscular Activation Patterns During Multidirectional Reaching in the Horizontal Plane, J. Neurophysiol. 103 (2010) 1532–1542. doi:10.1152/jn.00559.2009.

[64] H. Akaike, A new look at the statistical model identification, IEEE Trans. Automat. Contr. 19 (1974) 716–723. doi:10.1109/TAC.1974.1100705.

[65] G. Schwarz, Estimating the Dimension of a Model, Ann. Stat. 6 (1978) 461–464. doi:10.1214/aos/1176344136.

[66] L. Barnett, A.K. Seth, The MVGC multivariate Granger causality toolbox: A new approach to Granger-causal inference, J. Neurosci. Methods. 223 (2014) 50–68. doi:10.1016/j.jneumeth.2013.10.018.

[67] J. Cui, L. Xu, S.L. Bressler, M. Ding, H. Liang, BSMART: A Matlab/C toolbox for analysis of multichannel neural time series, Neural Networks. 21 (2008) 1094–1104. doi:10.1016/j.neunet.2008.05.007.

[68] N.M. López, F. di Sciascio, C.M. Soria, M.E. Valentinuzzi, Robust EMG sensing system based on data fusion for myoelectric control of a robotic arm, Biomed. Eng. Online. (2009). doi:10.1186/1475-925X-8-5.

[69] E. Taub, P. Perrella, G. Barro, Behavioral development after forelimb deafferentation on day of birth in monkeys with and without blinding, Science (80-.). (1973). doi:10.1126/science.181.4103.959.

[70] R. Colombo, F. Pisano, A. Mazzone, C. Delconte, S. Micera, M.C. Carrozza, P. Dario, G. Minuco, Design strategies to improve patient motivation during robot-aided rehabilitation, J. Neuroeng. Rehabil. 4 (2007) 3. doi:10.1186/1743-0003-4-3.

[71] J.W. Yoo, D.R. Lee, Y.J. Sim, J.H. You, C.J. Kim, Effects of innovative virtual reality game and EMG biofeedback on neuromotor control in cerebral palsy., Biomed. Mater. Eng. 24 (2014) 3613–8. doi:10.3233/BME-141188.

[72] H. Van de Meent, B.C.M. Baken, S. Van Opstal, P. Hogendoorn, Critical illness VR rehabilitation device (X-VR-D): Evaluation of the potential use for early clinical rehabilitation, J. Electromyogr. Kinesiol. 18 (2008) 480–486. doi:10.1016/j.jelekin.2006.11.005.

[73] T. Heo, K. Huang, H.J. Chizeck, Performance evaluation of haptically enabled sEMG, in: 2018 Int. Symp. Med. Robot., IEEE, 2018: pp. 1–6. doi:10.1109/ISMR.2018.8333289.

[74] C. Casellato, A. Pedrocchi, G. Zorzi, L. Vernisse, G. Ferrigno, N. Nardocci, EMG-Based Visual-Haptic Biofeedback: A Tool to Improve Motor Control in Children With Primary Dystonia, IEEE Trans. Neural Syst. Rehabil. Eng. 21 (2013) 474–480. doi:10.1109/TNSRE.2012.2222445.

[75] M.S. Cameirão, S. Bermúdez I Badia, E. Duarte Oller, P.F.M.J. Verschure, The

rehabilitation gaming system: a review., Stud. Health Technol. Inform. 145 (2009) 65–83. http://www.ncbi.nlm.nih.gov/pubmed/19592787.